

# Morphology of nanoporous germanium layers formed by implantation of $\text{Cu}^+$ , $\text{Ag}^+$ and $\text{Bi}^+$ ions of various energies

© T.P. Gavrilova, V.F. Valeev, V.I. Nuzhdin, A.M. Rogov, D.A. Konovalov, S.M. Khantimerov, A.L. Stepanov

Zavoisky Physical-Technical Institute, FRC Kazan Scientific Center of RAS,  
420029 Kazan, Russia  
e-mail: tatyana.gavrilova@gmail.com

Received November 4, 2023

Revised December 28, 2024

Accepted January 17, 2024

The formation of thin surface amorphous layers of nanoporous Ge of various morphologies due to the high-dose ion implantation of flat single-crystalline *c*-Ge substrates in the irradiation energy range 10–40 keV was investigated. The implantation was carried out with metal ions of different masses at the current density  $5 \mu\text{A}/\text{cm}^2$  and doses of  $1.0 \cdot 10^{17}$  ( $^{63}\text{Cu}^+$ ) and  $5.0 \cdot 10^{16}$  ( $^{108}\text{Ag}^+$   $^{209}\text{Bi}^+$ ) ion/ $\text{cm}^2$ . The morphology analysis of nanoporous structures was performed using high-resolution scanning electron microscopy. It was found that at low irradiation energies of 10 – 15 keV in the case of low mass ions such as  $^{63}\text{Cu}^+$  and  $^{108}\text{Ag}^+$  misoriented thin needle-shaped nanowires were created on the *c*-Ge surface, and in the case of  $^{209}\text{Bi}^+$  ions a porous layer consisting of densely packed intertwined nanowires was formed. At high energies of 30–40 keV, the morphology of nanoporous Ge changed its shape with increasing mass of the implanted ion sequentially from a three-dimensional network structure to a spongy one, consisting of single spatially separated thin intertwined nanowires.

**Keywords:** nanoporous germanium, ion implantation, surface morphology, ion distribution profiles.

DOI: 10.61011/JTF.2024.04.57532.276-23

## Introduction

Relatively recently in the papers [1–5] new abilities were demonstrated of effective use of thin nanoporous layers of germanium (*p*-Ge), formed by a low-energy implantation of the surface of single-crystal substrates *c*-Ge. *p*-Ge layers can be used as anti-reflective coatings to reduce optical losses and to increase efficiency of photon energy conversion into electrical signal in solar cells [1,2], to manufacture photodetectors of near IR ranges [3,4], as well as to create anodes of lithium ion batteries with high capacity that withstand without mechanical destruction a large number of charge/discharge cycles in electrolytes [5,6].

Structure and morphology features of *p*-Ge, such as specific surface area of nanopores, free volume, dimensional characteristics of nanostructure elements of pores, etc., if *p*-Ge layers are made by method of ion implantation, are determined by the main parameters and conditions of the technological process: energy *E*, dose *D*, current density *J*, temperature of irradiated matrix, mass of implanted ion [7,8].

Values of used radiation *E*, at which *p*-Ge layers which are usually formed, can be conditionally divided into several ranges. The highest *E* include values from tens MeV to GeV. Such range of *E* determines the so called implantation by most fast ions (SWIFT heavy ion irradiation (SHII)). In this case, *p*-Ge layer which formed deep from practically indestructible surface of the *c*-Ge substrate after the ion implantation, as a rule, for creation of *p*-Ge additional intensive thermal annealing is necessary, this was shown, for example, during irradiation of *c*-Ge by  $^{197}\text{Au}^{13+}$  ions with

$E = 185 \text{ MeV}$  [9] or  $^{108}\text{Ag}^+$  ions with  $E = 100 \text{ MeV}$  [10]. Further among the used *E* of wide range with lower values of  $\sim 50$  to  $500 \text{ keV}$  is outlined. Examples of such experiments can be founded in papers describing implantation by ions such as  $^{122}\text{Sb}^+$  with  $E = 200 \text{ keV}$  [11] or  $^{119}\text{Sn}^+$  with  $E = 150 \text{ keV}$  [12]. At lower *E*, *p*-Ge layers are formed with open surface pores. The next range comprises low *E* of  $\sim 10$  to  $50 \text{ keV}$ . Illustrations of these *E* are papers where *c*-Ge was irradiated by  $^{40}\text{Ar}^+$  [13] or  $^{119}\text{Sn}^+$  ions with  $E = 30 \text{ keV}$  [14]. Formation of surface nanostructures of various semiconductors at most low values  $E < 10 \text{ keV}$  of implantation with participation of surface effective sputtering is discussed in papers [15–19].

The present paper relates to issues of morphology type change of surface *p*-Ge layers formed during low-energy implantation with  $E = 10 - 40 \text{ keV}$  by metal ions of different mass such as  $^{63}\text{Cu}^+$ ,  $^{108}\text{Ag}^+$  and  $^{209}\text{Bi}^+$ .

## 1. Experimental procedure

The substrates for the ion implantation as smooth polished plates of *c*-Ge  $700 \mu\text{m}$  thick with crystal-lattice orientation (111). Implantation was performed at the selected most stable conditions of irradiation with  $E = 10, 20, 30$  and  $40 \text{ keV}$  for  $^{63}\text{Cu}^+$  at  $D = 1.0 \cdot 10^{17}$  ion/ $\text{cm}^2$  and  $E = 10, 15, 25$  and  $30 \text{ keV}$  for  $^{108}\text{Ag}^+$  with  $D = 5.0 \cdot 10^{16}$  ion/ $\text{cm}^2$  respectively. In accelerator ILU-3 with a normal angle of incidence of the ion beam on the surface *c*-Ge was used. For the heavier  $^{209}\text{Bi}^+$  ions stable, stable condition operation of the accelerator

was achieved only for two  $E = 15$  and  $35$  keV with  $D = 5.0 \cdot 10^{16}$  ion/cm<sup>2</sup>. For the comparative experiments the selection of ions for irradiation was determined by noticeable difference in their masses. Applied features of accelerator ILU-3 are described in detail [8]. Current density  $J$  during experiments was set  $5 \mu\text{A}/\text{cm}^2$ . Sample size was  $1 \times 1$  cm.

Morphology of formed surface layers was observed on a scanning electron microscope Merlin (Carl Zeiss) at accelerating voltage of probe electrons  $5$  keV and current  $300$  pA. This microscope was equipped with detector of electron backscattered diffraction (EBSD) HKL NordLys (Oxford Instruments). During EBSD the following modes were selected: accelerating voltage of electrons is also  $5$  keV, probe current is  $600$  pA, work distance between lens and sample surface is  $9.6$  mm. To reach the optimal conditions of experiment and to gather maximum number of reflected electrons on EBSD detector the sample was installed at angle  $70^\circ$  relative to normal of the incident flow probe electrons. Analysis of EBSD patterns was made using automated program complex Aztec-2.1. Reproducibility of the obtained results on monitoring the surface morphology of the surface  $c$ -Ge irradiated by various ions is ensured by reproducible measurements on series of samples prepared as result of several repeated experiments on ion implantation.

The ion implantation was performed in vacuum  $10^5$  mm Hg. During the electron microscopic observations possible rise of hydrocarbon contaminations on the irradiated surfaces of substrates Ge was not observed.

## 2. Results and discussions

To estimate profiles of distribution of the implanted ions in the near surface area of Ge sample irradiated by metal  $^{63}\text{Cu}^+$ ,  $^{108}\text{Ag}^+$  and  $^{209}\text{Bi}^+$  ions for values  $E = 10, 15, 20, 25, 30, 35$  and  $40$  keV, the free available computer program SRIM-2013 — ([www.srim.org](http://www.srim.org)) was used [20]. This program use model Monte Carlo for the statistical distribution of the implanted ions in the irradiated matrix Ge. In present calculations the sputtering of substrate Ge was not considered.

From the calculated profiles of the implanted ions in bulk of Ge for various values of  $E$  it follows that accumulation of metal atoms, occurred after the implanted ions neutralization, in the near surface region of the sample results in statistical distribution of impurity concentration along a Gaussian curve with maximum at depth of projection run  $R_p$ . Scattering of metal atoms depending on position of  $R_p$  is determined as  $\Delta R_p$ . Thickness of the implanted layer, as it is suggested to estimate [21], is  $h = R_p + 2\Delta R_p$ . Parameters  $R_p$ ,  $\Delta R_p$  and  $h$  for all values of  $E$ , corresponding to the case of Ge irradiation by  $^{63}\text{Cu}^+$ ,  $^{108}\text{Ag}^+$  and  $^{209}\text{Bi}^+$  ions were calculated. The exact numerical values will be given below in the text. Note also some common features resulting from the made modelling. When the ion mass increasing the depth of its penetration  $R_p$  into sample  $c$ -Ge decreases, and respectively the thickness of the implanted

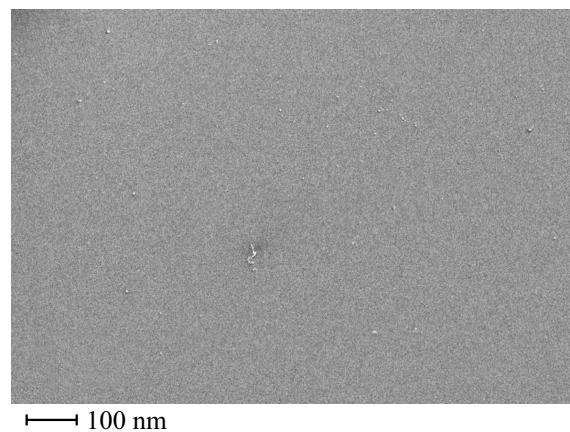


Figure 1. SEM image of unirradiated surface  $c$ -Ge.

layer also decreases. For example, it were estimated that for  $E = 30$  keV value  $h = 40.7$  nm for  $^{63}\text{Cu}^+$  and  $h = 28.2$  nm for  $^{108}\text{Ag}^+$ . With increase  $E$  value of  $h$  increases for all used ions. Thus, in case of  $^{209}\text{Bi}^+$  ions  $h$  increases from  $15.1$  to  $23.8$  nm upon  $E$  change from  $15$  to  $35$  keV respectively.

Fig. 1 shows SEM image of surface  $c$ -Ge before ion implantation. As seen, the surface is smooth, without any morphology nanoscale fragments. The present in image several defects are artifacts and determined by the dust deposited on sample, they were used for accurate focusing of the electron beam on the sample surface in SEM vacuum column.

According to data of EBSD from thin near surface layer of samples with thickness about  $10$  nm, determined by the projection range of electrons at minimum possible accelerating voltage in used SEM, all surface  $p$ -Ge layers formed by ion implantation are amorphous  $a$ -Ge and characterized by similar EBSD images. As example, Fig. 2 shows EBSD images of surface for unimplanted  $c$ -Ge substrate and sample irradiated by  $^{63}\text{Cu}^+$  ions with  $E = 10$  keV. For the virgin  $c$ -Ge, EBSD image (Fig. 2, *a*) comprises clear contrast crossing Kikuchi lines corresponding to structure of single-crystal  $c$ -Ge with orientation  $(100)$ . On the other hand, the diffraction pattern for the near surface layer of the implanted sample consists of blurred blind diffuse rings (Fig. 2, *b*). This indicates the surface amorphization during irradiation. Contribution to EBSD image from the implanted impurities in structure  $p$ -Ge is not shown.

As the most light ions in the present paper  $^{63}\text{Cu}^+$  were selected. SEM image of surface  $c$ -Ge, irradiated by  $^{63}\text{Cu}^+$  ions with various values of  $E = 10, 20, 30$  and  $40$  keV, are shown in Fig. 3. By contrast to smooth substrate  $c$ -Ge (Fig. 1) on the implanted samples  $\text{Cu}:p$ -Ge the formation of nanoporous layers of various morphology types was observed. At minimum value of  $E = 10$  keV on  $c$ -Ge sample in thin ( $h = 18.6$  nm) implanted layer the close-packed, disoriented in the surface plane short needle-shaped nanowires, not exceeding  $150$  nm in length with diameters up to  $20$  nm (Fig. 3, *a*) were formed. Practically there is no

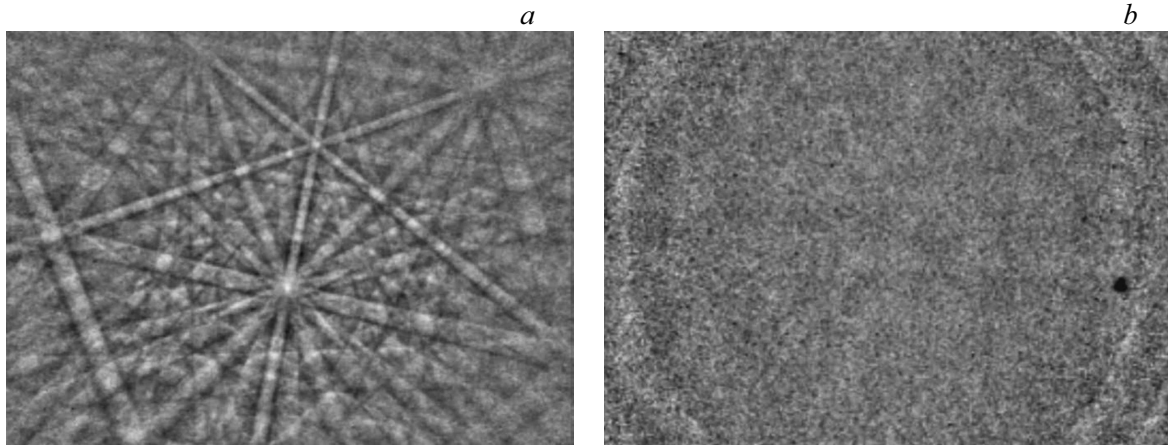


**Figure 2.** EBSD images of surface of unimplanted *c*-Ge (a) and *c*-Ge irradiated by  $^{63}\text{Cu}^+$  ions with  $E = 10\text{ keV}$  (b).

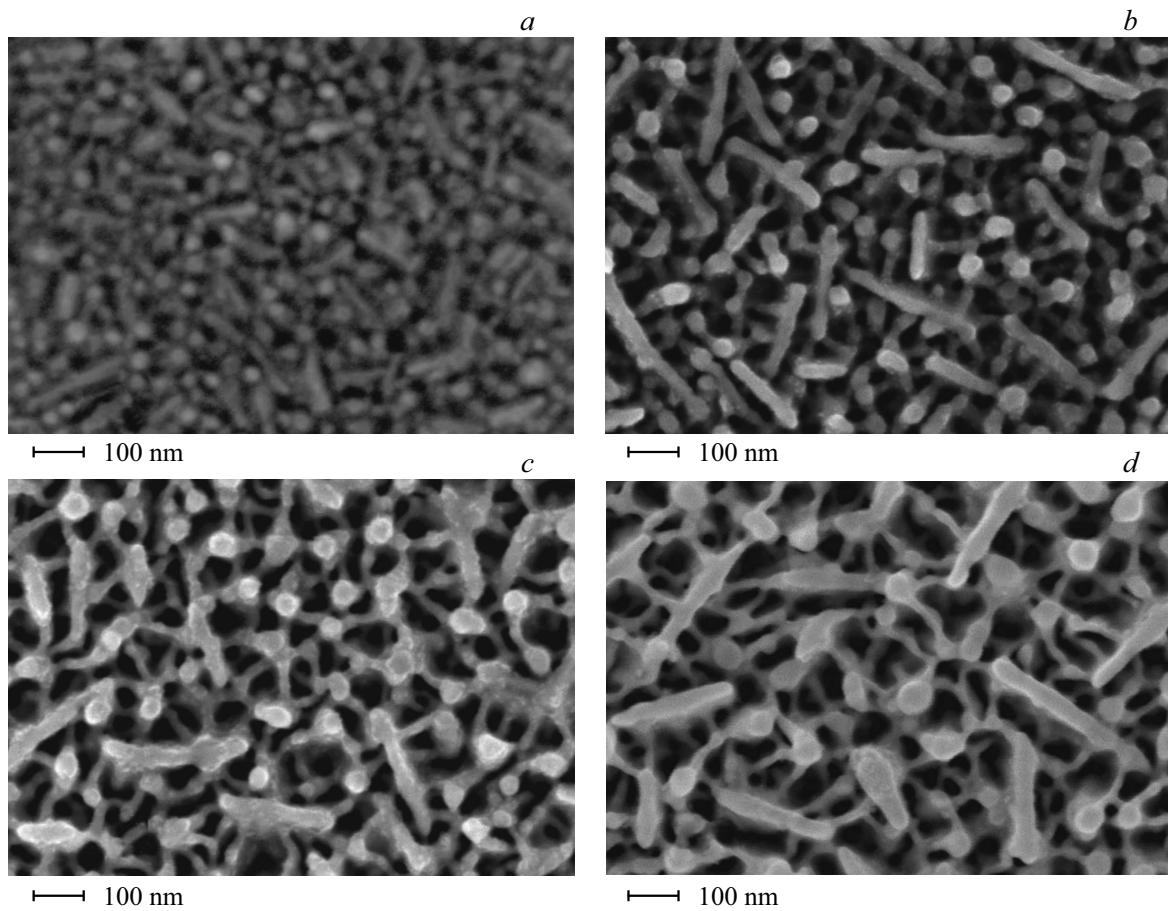


**Figure 3.** SEM image of surface *c*-Ge irradiated by  $^{63}\text{Cu}^+$  ions with  $D = 1.0 \cdot 10^{17}\text{ ion/cm}^2$  and  $J = 5\text{ }\mu\text{A/cm}^2$  with various irradiation  $E$ : 10 (a), 20 (b), 30 (c) and 40 keV (d).

free space between the needle-shaped nanowires. With  $E$  gradual increase to 40 keV there is increase in  $h$  to 50.5 nm, and quasi-one-dimensional needle structure (Fig. 3, a) is converted into a three-dimensional „neuron-like“ network layer *p*-Ge with nanoparticles in points connected by thin nanowires (Fig. 3, b–d). Diameters of the formed nanowires decrease with  $E$  increasing.

The first results on *p*-Ge-structure formation at surface of the *c*-Ge substrate in case of irradiation by  $^{63}\text{Cu}^+$  ions with  $E = 40\text{ keV}$  were described in paper [22]. At that a successive change on the morphology of layer *p*-Ge from hole honeycomb to 3D network with rise of  $D$  in range of  $1.8 \cdot 10^{15}$  to  $1.5 \cdot 10^{17}\text{ ion/cm}^2$  was observed. However, at the same time the needle formations oc-

curred at  $E = 10$  keV were not registered for higher  $E$ . As a whole for this type of composite material  $\text{Cu:p-Ge}$  it could be supposed the possibility that during ion implantation not only metal nanoparticles  $\text{Cu}$  are formed, but also nanofragments of  $\text{Cu}$  germanide. In practice the experimental confirmation of  $\text{Cu}$  germanide was not submitted. In this regard, studies by the method of photoelectron microscopy could be useful, till now they are not implemented for this type of samples  $\text{Cu:p-Ge}$ . Different compounds of germanium with  $\text{Cu}$  atoms synthesized by various methods, such as melting or sintering of appropriate chemical components, thermal decomposition in vacuum, electrolysis etc., were studied rather long [23] and stay under active intention currently [24–27]. In particular, paper [27] states that to form most stable phase  $\varepsilon_1\text{-Cu}_3\text{Ge}$  relatively high temperatures 250–400°C are required. Possibly for the formation of  $\text{Cu}$  germanide could be implemented during irradiation heated to appropriate temperatures of substrates  $c\text{-Ge}$  by ions  $^{63}\text{Cu}^+$ .

Fig. 4 shows SEM images of surface  $p\text{-Ge}$ -layers formed by implantation of the  $c\text{-Ge}$  substrate by  $^{108}\text{Ag}^+$  ions with various irradiation  $E$  10, 15, 25 and 30 keV. With  $E$  increasing change in morphology of nanostructured surface  $p\text{-Ge}$  was also observed. As in case of irradiation by  $^{63}\text{Cu}^+$  ions (Fig. 3, *a*) at  $E = 10$  keV the implanted layer  $\text{Ag:p-Ge}$  is characterized by the presence on sample surface of nanostructured needle formations of same size, chaotic oriented in place on the sample surface. At that the conditional value  $h$  for this layer is somewhat less than 14.3 nm. Opposite to SEM images in Fig. 3 for sample  $\text{Cu:p-Ge}$ , with increase in irradiation  $E$  to 30 keV the morphology of  $\text{Ag:p-Ge}$  layer is transformed not into 3D network structure (Fig. 3, *d*), but spongy layer with  $h = 28.2$  nm is formed comprising intertwined nanowires (Fig. 4, *d*). At that the nanowire diameters increase by more than two times with  $E$  increasing from 15 to 30 keV respectively.

The most previous studies on  $c\text{-Ge}$  irradiation by  $^{108}\text{Ag}^+$  ions with high  $D$  to  $10^{17}$  ion/cm<sup>2</sup>, resulting in  $p\text{-Ge}$  structures formation deep in bulk of matrix [28–31]. However, at that SHII ion implantation with  $E = 2.5$  and 100 MeV was used, which is not considered as case of low-energy irradiation considered here. The first statement which experimentally demonstrated the fundamental possibility of creating  $p\text{Ge}$  layer with nanoparticles of  $\text{Ag}$  layer during ion implantation with low  $E = 30$  keV and  $D = 7.5 \cdot 10^{16} - 1.5 \cdot 10^{17}$  ion/cm<sup>2</sup>, was presented in paper [32]. Later, by method of X-ray photoelectron spectroscopy it was shown [8] that no  $\text{Ag}$  germanides are not observed in the implanted layer  $\text{Ag:p-Ge}$  for the given irradiation conditions. This conclusion is confirmed by the state diagrams  $\text{Ag-Ge}$  [23] indicating that  $\text{Ag}$  germanides are formed at temperatures exceeding 600°C, i.e. in conditions that significantly differ from the performed ion implantation [33]. In context of the discussed system  $\text{Ag-Ge}$  it could be specify rather wide studies in creation of  $\text{AgGe}$  alloys in small range of proportions of their unmixed chemical components [33,34]. However, these alloys are

self-organized without the presence of  $\text{Ag}$  germanides in them.

Features of surface morphology difference of sample  $c\text{-Ge}$  implanted by  $^{209}\text{Bi}^+$  ions with irradiation  $E$  15 and 35 keV are shown in SEM images (Fig. 5) provided in two scales. At  $E = 15$  keV structure of surface layer  $\text{Bi:p-Ge}$  comprises densely packed intertwined nanowires with diameter 20–25 nm (Fig. 5, *a, b*). After increasing to  $E = 35$  keV the morphology of  $p\text{-Ge}$  changes, and structure becomes spongy-like, but at the same time the nanowire diameters significantly decrease to 8–10 nm. At that the intertwined nanowires are separated by distances up to 200 nm forming rather large voids between them (Fig. 5, *c, d*). In case of  $^{209}\text{Bi}^+$  ions the nanowires also are more thin and loosely packed as compared to somewhat more dense packed and thick nanowires in spongy-like layer  $\text{Ag:p-Ge}$  formed by irradiation by lighter  $^{108}\text{Ag}^+$  ions at  $E = 30$  keV (Fig. 4, *d*).

The history of  $c\text{-Ge}$  implantation by  $^{209}\text{Bi}^+$  ions resulting in formation of  $p\text{-Ge}$  layer begins from early papers [35,36], where irradiation was performed at high value of  $E = 280$  keV and  $D = 4.0 \cdot 10^{15}$  ion/cm<sup>2</sup>, which is beyond the conditions discussed herein. Further the results were presented for  $c\text{-Ge}$  irradiation by  $^{209}\text{Bi}^+$  ions with low  $E = 30$  and 60 keV at  $D = 5.0 \cdot 10^{13} - 5.0 \cdot 10^{17}$  ion/cm<sup>2</sup>, using the method of focused ion beam in electron microscope [37]. Authors [37] stated that with  $D$  increase in range  $1.0 \cdot 10^{14} - 5.0 \cdot 10^{17}$  ion/cm<sup>2</sup> change of  $p\text{-Ge}$  morphology was observed, in particular, size of pores in spongy structure of nanowires  $\text{Ge}$  increased. At that it could be concluded about saturation effect for both  $E$  at  $D = 5.0 \cdot 10^{16}$  ion/cm<sup>2</sup>, when it is achieved the morphology of pores and their size do not change. Paper [37] did not demonstrated information on used values of  $J$ , which does not allow to talk about the possible heating of samples during irradiation. This paper is more close to the results presented in present article, although lower  $E = 15$  keV were not used in [37]. Data obtained at higher values of  $E$  turn out to be similar, which confirms their authenticity.

Paper [23] state that  $\text{Bi}$  and  $\text{Ge}$  have equal mutual solubility in solid state at 250°C. Compounds  $\text{Ge}_{27}\text{Bi}_{37}$  are actively studied currently to create electrodes of  $\text{Mg}$ -ion batteries [38]. Implicitly,  $\text{Bi}$  germanides can be also formed in irradiated  $\text{Ge}$ , but this requires additional experimental check. However, in case of  $\text{Ge}$  mixing with  $\text{Bi}$  the situation became more serious due to large difference in melting point 938.2 and 271.4°C of corresponding chemical components as compared to cases of  $\text{Cu}$  and  $\text{Ag}$  characterized by melting points 1085 and 961.8°C, respectively.

Note that spongy layers  $\text{Ag:p-Ge}$  and  $\text{Bi:p-Ge}$  consisting of intertwined nanowires, shown in Fig. 4, *d* ( $^{108}\text{Ag}^+$ ) and 5, *c, d* ( $^{209}\text{Bi}^+$ ) for  $E = 30$  and 35 keV respectively, are formed during implantation with  $c\text{-Ge}$ -ions with mass comparable or exceeding the mass of  $^{108}\text{Ag}^+$  ions. Structures similar by morphology with  $\text{Ag:p-Ge}$  [39,40] were also observed for other heavy ions with intermediate masses, for example, for  $^{115}\text{In}^+$  [2],  $^{119}\text{Sn}^+$  [14] and  $^{122}\text{Sb}^+$  [41] ions

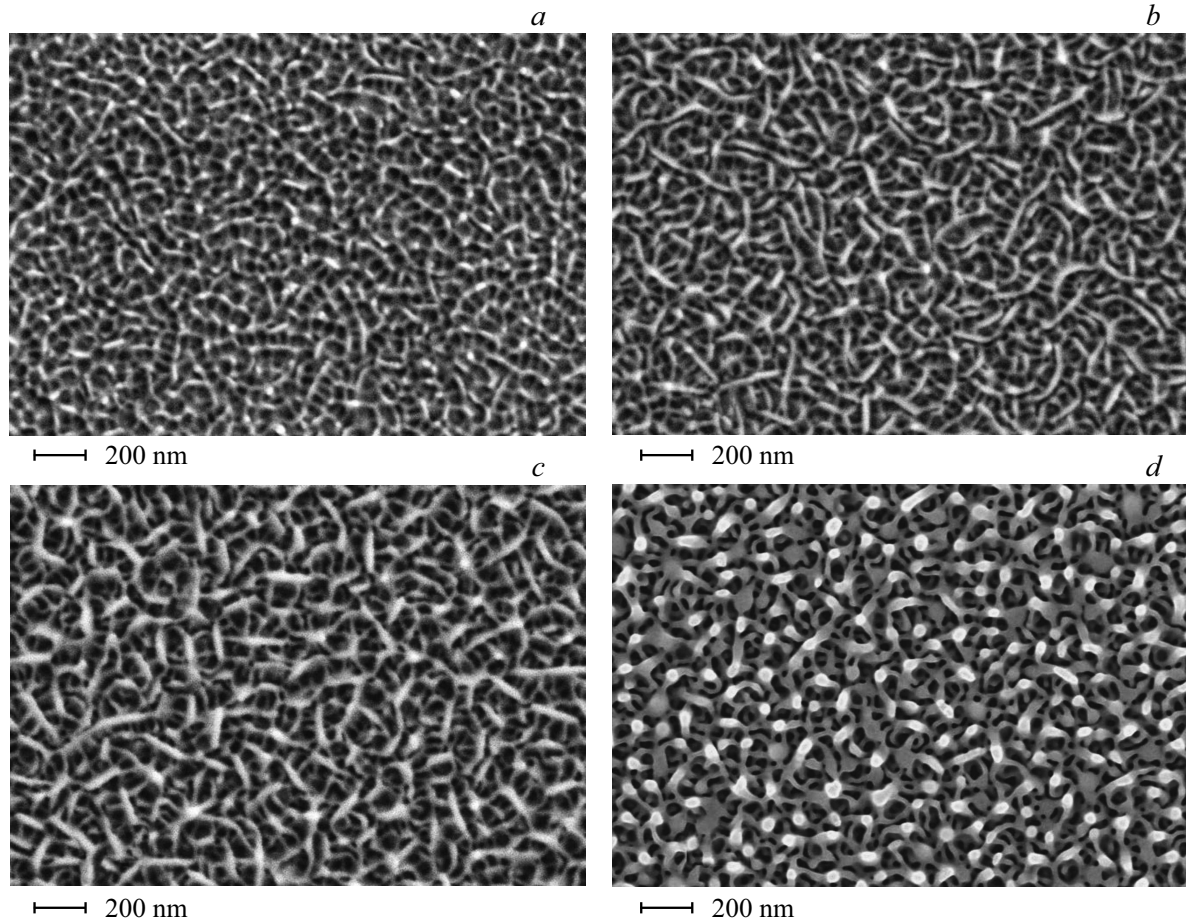


**Figure 4.** SEM image of surface *c*-Ge irradiated by  $^{108}\text{Ag}^+$  ions at  $D = 5.0 \cdot 10^{16} \text{ ion/cm}^2$  and  $J = 5 \mu\text{A/cm}^2$  with various irradiation  $E$ : 10 (a), 15 (b), 25 (c) and 30 keV (d).

at  $E = 30 \text{ keV}$ . However, issues of In and Sn germanides formation during ion implantation also were not discussed in publications.

As it was discussed in detail in monograph [8], during last fifty years, approximately, the studies of structural and morphology changes of ion implanted surface of Ge were performed. Nevertheless, the exact mechanisms of formation of various morphology types of *p*-Ge layers during ion irradiation are still unknown in spite of wide studies, accumulation of rich experimental material and fundamental understanding of a number of individual processes accompanying the phenomenon of pore formation [7,11]. Currently, in scientific publications two main priority and fundamentally different mechanisms are discussed, they describe the formation of *p*-Ge during ion irradiation. The first model is conventionally called „cluster-vacancy mechanism“, the other is explained by the theory of microexplosions. Besides, nanostructuring of surface during ion implantation also occurs as a result of effective sputtering with further re-deposition of the material, described in detail in papers [16,42]. In the development of the theory of sputtering a descriptive approach was suggested to form nanoporous layers, especially, for the case of lower

$E < 5 \text{ keV}$  of irradiation. In these papers a conclusion was also made on the significant role of local heating of the implanted materials in region of the ion tracks near the surface, which facilitates its effective sputtering and stimulation of pores formation.

The cluster-vacancy mechanism of *p*-Ge formation means combination of radiation-generated vacancies and their clusters occurring during impact collision of impurity ions with atoms of the irradiated matrix [43–46]. This mechanism action is based on the supposition of low efficiency of recombination of generated vacancies. Under these conditions the limit of solubility of vacancies is exceeded, resulting in their saturation in the implanted layer. With  $D$  increasing the vacancies and their clusters during diffusion in interstices combine into microscopic voids, as, for example, this is discussed in the paper [47] for the case of implantation by  $^{73}\text{Ge}^+$  ions with  $E = 300 \text{ keV}$  and  $D = 4 \cdot 10^{16} \text{ ion/cm}^2$ , excluding the ion synthesis process. As irradiation  $D$  increases, the concentration of microscopic voids increases to some value, and they merge forming macro- and macroscopic volume and surface voids — porous layer *p*-Ge. It was stated that *p*-Ge layers can be formed by ion irradiation not only of *c*-Ge, but also

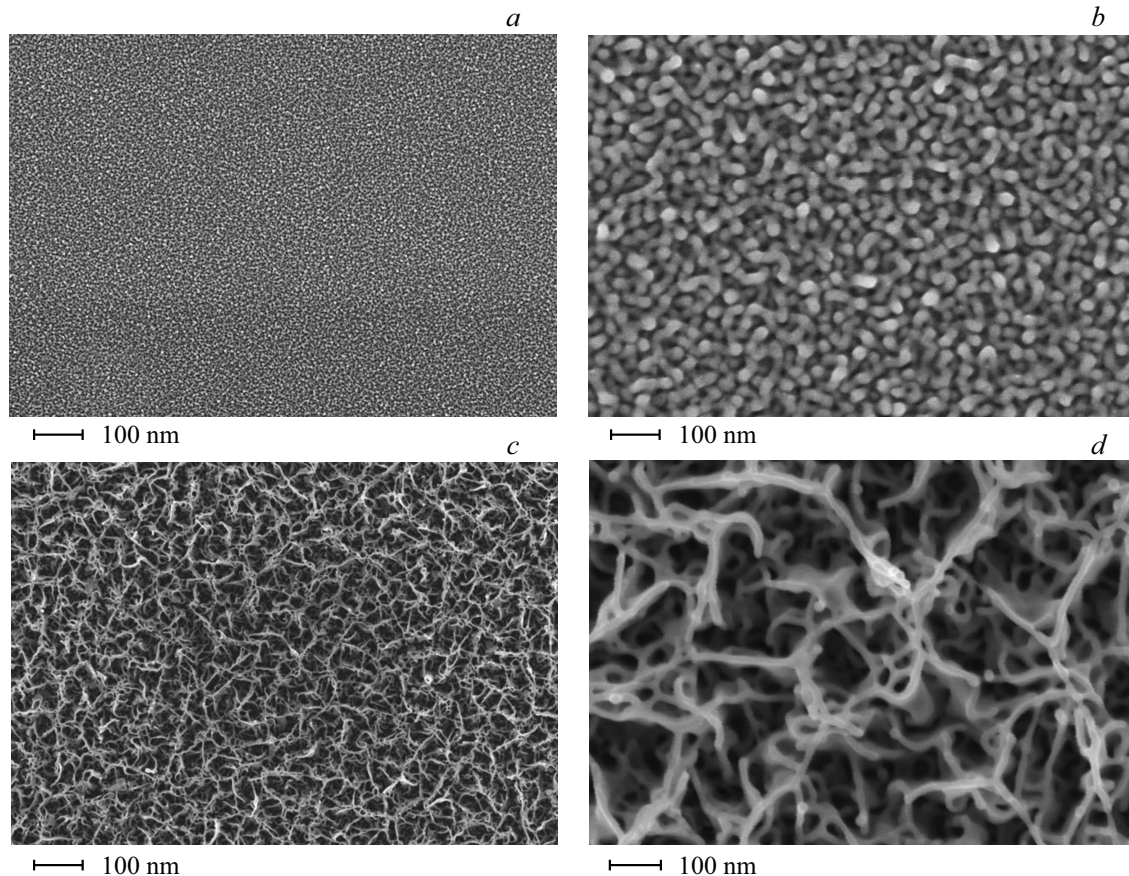


**Figure 5.** SEM image of surface  $c\text{-Ge}$  irradiated by  $^{209}\text{Bi}^+$  ions at  $D = 5.0 \cdot 10^{16} \text{ ion/cm}^2$  and  $J = 5 \mu\text{A/cm}^2$  with various irradiation  $E$ : 15 ( $a, b$ ) and 35 keV ( $c, d$ ).

of amorphous layer  $a\text{-Ge}$  [47–49]. However, paper [11] states that in contrast to the sputtering process, which results in surface atoms removal, the nanopores formation is determined by law of mass conservation, and effect of sputtering in the pore formation mechanism can be excluded. Correctness of this opinion is confirmed by paper [14], where  $p\text{-Ge}$  layer was formed during the ion implantation under thin surface protective film on  $c\text{-Ge}$  made of silicon nitride. Mechanism, based on the theory microexplosions [50], initially suggested for the case of metals irradiation [51], supposes the occurrence of nanopores during ion implantation of Ge as result of occurrence of heat peaks and deformation waves (pressure waves), formed during irradiation by overlap of generated ion cascades. As a result of collision of deformation waves there are microexplosions in the near surface region of Ge. Model of vacancies clusterization is determined generally by inefficiency of recombinations of point defects and vacancies occurrence, at the same time the material ability to experience micro-fractures during ion implantation of beam depends on mass and energy of ions, strength of interatomic bond, melting point, atomic density, average atomic mass, etc.

It was also stated, the pore formation process depends on conditions and parameters of ion implantation. However,

during discussion of mechanisms of  $p\text{-Ge}$  formation, as a rule, it is neglect the chemical interaction of the implanted ions and matrix Ge with formation of various composition compounds — germanides. This is due to that some papers state  $p\text{-Ge}$  formation during  $c\text{-Ge}$  irradiation by ions  $^{73}\text{Ge}^+$ , for example, [8,44,45]. Discussion and review of papers on the formation of various morphology forms of  $p\text{-Ge}$ , shown herein, with high degree of probability can suppose situations when during ion implantation in structure  $p\text{-Ge}$  chemical compounds — germanides can be formed. More over, may be these formed fragments of germanides determine the type of morphology structures together with the selected conditions of ion implantation. Thus, the authors of the present paper attract attention to wide problem on germanides formation in Ge implanted layers by method of ion implantation in the near surface Ge layers.

## Conclusion

Experimental results obtained in the paper demonstrate the formation of thin amorphous  $p\text{-Ge}$  layers with various morphology as a result of high-dose irradiation of single-crystal substrates  $c\text{-Ge}$  by ions of metals such as  $^{63}\text{Cu}^+$ ,

$^{108}\text{Ag}^+$  and  $^{209}\text{Bi}^+$  with energy  $E = 10 - 40$  keV. It is shown that at low irradiation  $E$  depending on mass of ions on surface  $c$ -Ge needle nanowires ( $^{63}\text{Cu}^+$  and  $^{108}\text{Ag}^+$ ) or layer of dense packed nanowires ( $^{209}\text{Bi}^+$ ) are formed. At high  $E$  the morphology of thin surface layers of nanoporous Ge with increasing on the mass of implanted ion changes its form successively from 3D network ( $^{63}\text{Cu}^+$ ) to spongy ( $^{108}\text{Ag}^+$  and  $^{209}\text{Bi}^+$ ), formed by individual with large spacing intertwined nanowires. So, for possible explanation of formation of various morphology forms of  $p$ -Ge it is necessary to discuss the conditions and parameters of ion irradiation of  $c$ -Ge such as  $E$  and mass of implanted ion, which was made in paper, and other factors shall be also considered.

## Funding

Creation and study of amorphous layers of nanoporous germanium  $\text{Ag}:p\text{-Ge}$  and  $\text{Cu}:p\text{-Ge}$  were financed by the grant of Russian Scientific Foundation № 19-79-10216. Studies of amorphous layers of nanoporous germanium  $\text{Bi}:p\text{-Ge}$  were performed with the financial support from the government assignment for FRC Kazan Scientific Center of RAS.

## Conflict of interest

The authors declare that they have no conflict of interest.

## References

- [1] D.P. Datta, T. Som. *Solar Energy*, **223**, 367 (2021). DOI: 10.1016/j.solener.2021.05.016
- [2] A.L. Stepanov, V.I. Nuzhdin, V.F. Valeev, D.A. Konovalov, A.M. Rogov. *Tech. Phys. Lett.*, **49** (4), 51 (2023). DOI: 10.21883/TPL.2023.04.55878.19466
- [3] D. Caudevilla, S. Algaidy, F. Perez-Zenteno, S. Duarte-Cano, R. Garsia-Hemme, E. San Andres, A. del Prado, R. Barrio, I. Torres, E. Garcia-Hemme, D. Pastor. *Semicond. Sci. Technol.*, **37**, 124001 (2022). DOI: 10.1088/1361-6641/ac9a67
- [4] H.H. Gandhi, D. Pastor, T.T. Tran, S. Kalchmair, L.A. Smile, J.P. Mailoa, R. Milazzo, E. Napolitani, M. Loncar, J.S. Williams, M.J. Aziz, E. Mazur. *Phys. Rev. Lett.*, **14**, 64051 (2020). DOI: 10.1103/PhysRevApplied.14.064051
- [5] N.G. Rudawski, B.L. Darby, B.R. Yates, K.S. Jones, R.G. Elliman, A.A. Volinsky. *Appl. Phys. Lett.*, **100**, 83111 (2012).
- [6] T.P. Gavrilova, S.M. Khantimerov, V.I. Nuzhdin, V.F. Valeev, A.M. Rogov, A.L. Stepanov. *Tech. Phys. Lett.*, **48** (4), 70 (2022). DOI: 10.21883/TPL.2022.04.53488.19096
- [7] N.G. Rudawski, K.S. Jones. *J. Mater. Res.*, **28** (13), 1633 (2013). DOI: 10.1557/jmr.2013.24
- [8] A.L. Stepanov, V.I. Nuzhdin, A.M. Rogov, V.V. Vorobiev, *Formirovanie sloev poristogo kremniya i germaniya s metallichesкими nanochasticami* (FITs KazNTs RAN, Kazan, 2019) (in Russian).
- [9] M.C. Ridgway, T. Bierschenk, R. Giilian, B. Afra, M.D. Rodriguez, L.L. Araujo, A.P. Byrne, N. Kirby, P.H. Pakerinen, F. Djurabekova, K. Nordlund, M. Schleberger, O. Osmani, N. Mendeleev, B. Rethfeld, P. Kluth. *Phys. Rev. Lett.*, **110**, 245502 (2013).
- [10] S. Hooda, S.A. Khan, B. Satpati, D. Kanjilal, D. Kabiraj. *Appl. Phys. Lett.*, **108**, 201603 (2016).
- [11] T. Lohner, A. Németh, Z. Zolnai, B. Kalas, A. Romanenko, N.Q. Khánh, E. Szilágyi, E. Kótai, E. Agócs, Z. Tóth, J. Budai, P. Petrik, M. Fried, I. Bársony, J. Gyulai. *Mater. Sci. Semicond. Proc.*, **152**, 107062 (2022). DOI: 10.1016/j.mssp.2022.107062
- [12] S. Prucnal, J. Zuk, R. Hübner, J. Duan, M. Wang, K. Pysznik, A. Drozdziel, M. Turek, S. Zhou. *Materials*, **13**, 1408 (2020). DOI: 10.3390/ma13061408
- [13] S.-Y. Wen, L. He, Y.-H. Zhu, J.-W. Luo. *J. Appl. Phys.*, **133**, 45703 (2023). DOI: 10.1063/5.0134924
- [14] D. Chowdhury, S. Mondal, M. Secchi, M.C. Giordano, L. Vanzetti, M. Barozzi, M. Bersani, D. Giubertoni, F.B. de Mongeot. *Nanotechnol.*, **33**, 305304 (2022). DOI: 10.1088/1361-6528/ac64ae
- [15] X. Ou, A. Keller, M. Helm, J. Fassbender, S. Facko. *Phys. Rev. Lett.*, **111**, 16101 (2013). DOI: 10.1103/PhysRevLett.111.016101.
- [16] Y. Kudriavtsev, A. Hernandez-Zanabria, C. Salinas, R. Asomoza. *Vacuum*, **177**, 109393 (2020). DOI: 10.1016/j.vacuum.2020.109393
- [17] Y. Kudriavtsev, R. Asomoza, A. Hernandez, D.Y. Kazantsev, B.Y. Ber, A.N. Gorokhov. *J. Vacuum Sci. Technol. A*, **38**, 53203 (2020). DOI: 10.1116/6.0000262
- [18] M.A. Smirnova, A.S. Ivanov, V.I. Bachurin, A.B. Churilov. *J. Phys. Conf. Ser.*, **2086**, 12210 (2021). DOI: 10.1088/1742-6596/2086/1/012210
- [19] L. Vázquez, A. Redondo-Cubero, K. Lorentz, F.J. Palomares, R. Cuerno. *J. Phys. Conens. Matter.*, **34**, 333002 (2022). DOI: 10.1088/1361-648X/ac75a1
- [20] J.F. Ziegler, M.D. Ziegler, J.P. Biersack. *Nucl. Instr. Meth. Phys. Res. B*, **268**, 1818 (2010). DOI: 10.1016/j.nimb.2010.02.091
- [21] M. Nastasi, J.W. Mayer, J.K. Hirvonen. *Ion-solid Interactions* (Cambridge Univ. Press: Cambridge, 1996), 540 p.
- [22] A.M. Rogov, V.I. Nuzhdin, V.F. Valeev, I.A. Romanov, I.M. Klimovich, A.L. Stepanov. *Nanotechnologies in Russia*, **13** (9–10), 487 (2019).
- [23] G.V. Samsonov, Y.N. Bondarev, Germanides (Springer, Berlin, 1969), 163 p.
- [24] C. Furgeaud, L. Simont, A. Michel, G. Abadias. *Acta Mater.*, **159**, 286 (2018). DOI: 10.1016/j.actamat.2018.08.019
- [25] E.M. Smith, W.H. Streyer, N. Nader, S. Vangala, G. Grzybowski, R. Soref, D. Wasserman, J.W. Cleary. *Opt. Mater. Express*, **8** (4), 319998 (2018). DOI: 10.1364/OME.8.000968
- [26] C. Shang, L. Hu, D. Luo, K. Kempa, Y. Zhang, G. Zhou, X. Wang, Z. Chen. *Adv. Sci.*, **7**, 2002358 (2020). DOI: 10.1002/advs.202002358
- [27] M.O. Aboelfotoh, M.A. Borek, J. Narayan. *J. Appl. Phys.*, **87** (1), 365 (2000).
- [28] T. Steinbach, J. Wernecke, P. Kluth, M.C. Ridgway, W. Wesch. *Phys. Rev. B*, **84**, 104108 (2011). DOI: 10.1103/PhysRevB.84.104108
- [29] S. Hooda, S.A. Khan, B. Satpati, A. Uedono, S. Sellaiyan, K. Asokan, D. Kanjilal, D. Kabiraj. *Microporous Mesoporous Mater.*, **225**, 323 (2016). DOI: 10.1016/j.micromeso.2016.01.006

- [30] S. Hooda, S.A. Khan, B. Satpati, D. Kanjilal, D. Kabiraj. Appl. Phys. Lett., **108**, 201603 (2016). DOI: 10.1063/1.4950710
- [31] S. Hooda, S.A. Khan, B. Satpati, D. Stange, D. Buca, M. Bala, C. Pannu, D. Kanjilal, D. Kabiraj. Appl. Phys. A, **122**, 227 (2016). DOI: 10.1007/s00339-016-9776-5
- [32] A.L. Stepanov, V.V. Vorobev, M.A. Ermakov, V.F. Valeev, V.I. Nuzhdin. Scientific J. Microelectron., **4** (3), 11 (2014).
- [33] S. Delsante, G. Borzone, R. Novakovic. Thermochemica Acta, **682**, 178432 (2019). DOI: 10.1016/j.tca.2019.178432
- [34] D. Manasijevic, L. Balanovic, I. Markovic, M. Gorgievski, U. Stamenkovic, D. Minic, M. Premovic, A. Dordevic, V. Cosovic. J. Thermak. Analysis Calorimetry, **147**, 1995 (2022). DOI: 10.1007/s10973-021-10664-y
- [35] B.R. Appleton, O.W. Holland, J. Narayan, O.E. Schow III, J.S. Williams, K.T. Short, L. Lawson. Appl. Phys. Lett., **41** (8), 711 (1982). DOI: 10.1063/1.93643
- [36] O.W. Holland, B.R. Appleton, J. Narayan. J. Appl. Phys., **54** (5), 2295 (1983). DOI: 10.1063/1.332385
- [37] L. Bischoff, W. Pilz, B. Schmidt. Appl. Phys. A, **104**, 1153 (2011). DOI: 10.1007/s00339-011-6396-y
- [38] Z. Zhang, M. Song, C. Si, W. Cui, Y. Wang. Science, **3**, 100070 (2023). DOI: 10.1016/j.esci.2022.07.004
- [39] A.L. Stepanov, B.F. Farrakhov, Ya.V. Fattakhov, A.M. Rogov, D.A. Konovalov, V.I. Nuzhdin, V.F. Valeev. Vacuum, **186**, 110060 (2021). DOI: 10.1016/j.vacuum.2021.110060
- [40] A.L. Stepanov, S.M. Khantimerov, V.I. Nuzhdin, V.F. Valeev, A.M. Rogov. Vacuum, **194**, 110552 (2021). DOI: 10.1016/j.vacuum.2021.110552
- [41] A.M. Rogov, V.I. Nuzhdin, V.F. Valeev, A.L. Stepanov. Composit. Comm., **19**, 6 (2020). DOI: 10.1016/j.coco.2020.01.002
- [42] P. Bellon, S.J. Chey, J.E. van Nostrand, M. Ghaly, D.G. Cahill, R.S. Averback. Surf. Sci., **339** (1–2), 135 (1995). DOI: 10.1016/0039-6028(95)00656-7
- [43] J.C. Kim, D.G. Cahill, R.S. Averback. Surf. Sci., **574** (2–3), 175 (2005). DOI: 10.1016/j.susc.2004.10.026
- [44] I.H. Wilson. J. Appl. Phys., **53**, 1698 (1982). DOI: 10.1063/1.221636
- [45] I.D. Desnica-Frankovic, P. Dubcek, U.V. Desnica, S. Bernstorff, M.C. Ridgway, C.J. Glover. Nucl. Instr. Meth. Phys. Res. B, **249** (1–2), 114 (2006). DOI: 10.1016/j.nimb.2006.03.093
- [46] G. Impellizzeri, L. Romano, L. Bosco, C. Spinella, M.G. Grimaldi. Appl. Phys. Express, **5**, 35201 (2012).
- [47] L. Romano, G. Impellizzeri, M.V. Tomasello, F. Giannazzo, C. Spinella, M.G. Grimaldi. J. Appl. Phys., **107**, 84314 (2010).
- [48] I.M. Klimovich, A.L. Stepanov. Lett. Mater., **13** (3), 243 (2023). DOI: 10.22226/2410-3535-2023-3-243-248
- [49] A.V. Pavlikov, A.M. Rogov, A.M. Sharafutdinova, A.L. Stepanov. Vacuum, **184**, 109881 (2021). DOI: 10.1016/j.vacuum.2020.10988
- [50] M. Ghaly, K. Nordlund, R.S. Averback. Philosoph. Magazin, **79**, 795 (1999).
- [51] C. Cawthorne, E.J. Fulton. Nature, **216**, 575 (1967).

*Translated by D.Kondaurov*